Journal of the European Ceramic Society 21 (2001) 2723–2730

www.elsevier.com/locate/jeurceramsoc

The effect of partial isovalent substitution in the A-sublattice on MW properties of materials based on $Ba_{6-x}Ln_{8+2x/3}Ti_{18}O_{54}$ solid solutions

A.G. Belous[a,*], O.V. Ovchar[a], M. Valant[b], D. Suvorov[b], D. Kolar[b]

[a]*Department of Solid State Chemistry, V.I. Vernadskii Institute of General and Inorganic Chemistry, NAS of Ukraine, 32-34 Palladin avenue, 252680 Kyiv 142, Ukraine*

[b]*"Jožef Stefan" Institute, Jamova 39, 1000 Ljubljana, Slovenia*

Abstract

Investigations of materials based on the three systems: $(Ba_{1-y}Pb_y)_{6-x}La_{8+2x/3}Ti_{18}O_{54}$, $(Ba_{1-y}Pb_y)_{6-x}Nd_{8+2x/3}Ti_{18}O_{54}$, and $(Ba_{1-y}Ca_y)_{6-x}Ln_{8+2x/3}Ti_{18}O_{54}$ revealed that a partial isovalent substitution in cation sublattices allows the control of the electro-physical parameters of microwave dielectrics. The investigations were carried out over a wide range of x values. Data on the relationship between the crystal-cell parameters and the microwave dielectric properties (ε, Q, and t_f) have been obtained and related to the size of the isovalent ion residing at crystallographic sites in the A-sublattice. Based on the data obtained, a non-random distribution of Ca^{2+} and Pb^{2+} ions on different A-sites as a function of their concentration in different systems was concluded. Various temperature-stable microwave dielectrics, based on the above three systems, have been synthesized and shown to exhibit excellent MW properties.

Keywords: Dielectric properties; Functional applications; Perovskites; Sintering; X-ray methods

1. Introduction

The continuing interest in investigations of $Ba_{6-x}Ln_{8+2x/3}Ti_{18}O_{54}$ solid solutions, where Ln = La–Gd, is a consequence of the unique dielectric properties of these materials. A combination of high dielectric constant ($\varepsilon \approx 70$–100), low dielectric losses, and high temperature stability of the permittivity makes them very important for applications in communication devices. However, the requirements of modern communication technologies results in growing demands for further enhancements in the performance of materials. With materials based on $Ba_{6-x}Ln_{8+2x/3}Ti_{18}O_{54}$ solid solutions, the main engineering goal is the suppression of the temperature coefficient of resonant frequency (τ_f), which is related to the temperature coefficient of dielectric constant (τ_ε) by the equation $\tau_f = -\tau_\varepsilon/2 - \alpha$ (where α is the linear thermal expansion coefficient), to almost zero ppm/K while retaining high Q-values and a high dielectric constant. The electro-physical characteristics (ε, τ_f, Q) of $Ba_{6-x}Ln_{8+2x/3}Ti_{18}O_{54}$ solid solutions are sensitive to both x value and rare-earth ion.[1,2] Typically, by decreasing x or increasing the rare-earth ionic radii the dielectric constant and the dielectric losses within the solid solubility range increase. In addition, partial isovalent substitution in the cation sublattice can have a significant effect on the electro-physical properties of these materials.[3–6] The goal of this study is to investigate isovalently substituted La, Nd, and Sm-containing $Ba_{6-x}Ln_{8+2x/3}Ti_{18}O_{54}$ solid solutions over a wide ranges of x values and substituent concentration.

2. Experimental procedure

The powders were synthesized by a solid-state reaction technique. Extra-pure $BaCO_3$, $CaCO_3$, Sm_2O_3, Nd_2O_3, La_2O_3, TiO_2 and $PbTiO_3$ were used as the starting reagents. These starting reagents were mixed and ball milled: the mixture was then dried and calcined at 1150–1200 °C for 2–3 h. $PbTiO_3$ powder was added at the second stage of calcination to minimize the PbO evaporation. Pre-reacted powders were pressed into pellets and sintered at 1330–1380 °C for 2–3 h. The phase composition and lattice parameters of the materials were analyzed by powder X-ray diffraction (XRD) using

* Corresponding author. Tel.: +380-44-4442-211; fax: +380-44-4442-211.

E-mail address: belous@mail.kar.net (A.G. Belous).

0955-2219/01/$ - see front matter
PII: S0955-2219(01)00352-1

a "DRON 4" diffractometer and Cu K_α radiation. Microstructures of the ceramics were examined and microanalyses were performed by SEM (Jeol JXA 840A, Tracor Series II). The electro-physical characteristics of the ceramic samples were examined at frequencies around 10 GHz. The dielectric constant (ε) and dielectric losses (tg δ) of the materials were measured using a modified-dielectric-resonator method.[7] Dielectric losses of the materials were estimated from the frequency dependence of the transfer constant in the vicinity of the resonant frequency (f_{res}). The temperature behaviour of the dielectric constant was evaluated from the temperature dependence of f_{res}.

3. Results and discussion

3.1. The $(Ba_{1-y}Pb_y)_{6-x}Nd_{8+2x/3}Ti_{18}O_{54}$ system

The phase composition of the $(Ba_{1-y}Pb_y)_{6-x}Nd_{8+2x/3}Ti_{18}O_{54}$ system was examined at $x=0$, 0.75, and 1.5. Based on XRD investigations, the single-phase region was determined to exist within the Pb^{2+} concentration range corresponding to $0<y\leqslant 0.70$ ($x=0$), $0<y<0.60$ ($x=0.75$), $0<y\leqslant 0.4$ ($x=1.5$). For this last case the results are in good agreement with those obtained by Podlipnik et al.[5] For all compositions outside the single-phase region a secondary phase was detected and identified as $Nd_4Ti_9O_{24}$. Fig. 1 shows the X-ray diffraction patterns of the $(Ba_{1-y}Pb_y)_{6-x}Nd_{8+2x/3}Ti_{18}O_{54}$ ceramic samples with the highest Pb^{2+} concentration: $y=0.70$ ($x=0$), $y=0.65$ ($x=0.75$), and $y=0.5$ ($x=1.5$). In the case $x=1.5$ and $y=0.5$ (multiphase region), the peaks corresponding to $Nd_4Ti_9O_{24}$ are clearly visible whereas in the case $x=0.75$ and $y=0.65$ (multiphase region close to the ss. limit) only faint traces of the most intense peaks of $Nd_4Ti_9O_{24}$ could be recognized on the XRD plot. When $x=0$ and $y=0.70$ (single-phase region) the peaks of $Nd_4Ti_9O_{24}$ are not present or their intensity is below the XRD sensitivity (Fig. 1). A typical influence of the lead concentration on the lattice parameters of the $(Ba_{1-y}Pb_y)_{6-x}Nd_{8+2x/3}Ti_{18}O_{54}$ solid solutions is shown in Fig. 2 for the $x=0.75$ system. With an increase of the Pb^{2+} concentration the crystal-lattice parameters (c and b) decrease monotonically up to the solid-solubility limits indicated by the powder XRD patterns. Typically, Pb incorporation has only a slight influence on the dimensions of the *a*-axis.

In addition to XRD analysis, SEM microstructural investigations and microanalyses of the $(Ba_{1-y}Pb_y)_{6-x}Nd_{8+2x/3}Ti_{18}O_{54}$ ceramic samples have been performed. Unlike XRD, the microstructural analysis revealed a secondary TiO_2 phase, the concentration of which is very low for small values of y, but increases with an increase in y (Fig. 3). The appearance of this phase is related to the evaporation of lead during heat treatment, as already reported by Podlipnik et al.,[5] and does not indicate that the solid-solubility limit is being exceeded. As a result, only nominal Pb concentrations are reported in this study. Therefore, when taking into account the XRD and SEM data and the evaporation of lead we cannot be absolutely certain that the solid-solubility limits for Pb^{2+} ions correspond to $y=0.70$ ($x=0$), $y=0.60$ ($x=0.75$) and $y=0.4$ ($x=1.5$). Nevertheless, the substitutional experiments have shown that the solid-solubility limits are close to these values and that by decreasing the value of x in $(Ba_{1-y}Pb_y)_{6-x}Nd_{8+2x/3}Ti_{18}O_{54}$ the solid-solubility region for Pb^{2+} incorporation becomes wider.

The crystal structure of $Ba_{6-3x}R_{8+2x}Ti_{18}O_{54}$ solid solutions includes elements of tungsten bronze with channels extending in the short-axis direction. Corner-sharing TiO_6 octahedra form a network with three types of channels: pentagonal, tetragonal and triangular. Rare-earth ions occupy the rhombic channels, Ba ions completely fill the pentagonal channels (for $x<2$), while the remaining Ba ions share the rhombic channels. The triangular channels are empty. The structural formula may be presented as $[Ln_{8+2x/3}Ba_{2-x}V_{x/3}][Ba_4]Ti_{18}O_{54}$,

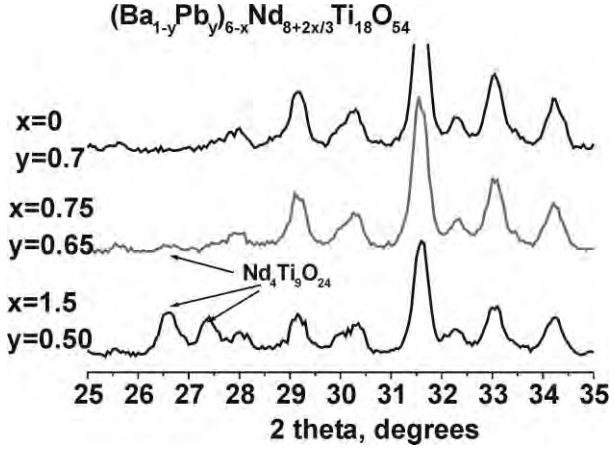

Fig. 1. X-ray diffraction patterns of the $(Ba_{1-y}Pb_y)_{6-x}Nd_{8+2x/3}Ti_{18}O_{54}$ system.

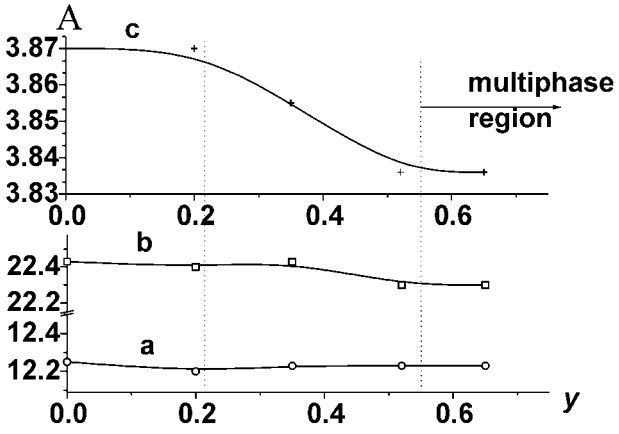

Fig. 2. Lattice parameters of the $(Ba_{1-y}Pb_y)_{6-x}Nd_{8+2x/3}Ti_{18}O_{54}$ system with $x=0.75$ as a function of Pb^{2+} concentration.

where V represents structural vacancies.[2] In the first square brackets, the cations located at the tetragonal sites of the perovskite blocks are shown and in the second the cations located at the pentagonal sites. Earlier, when examining the composition $Ba_{3.5}PbNd_9Ti_{18}O_{54}$ ($x=1.5$ and $y=0.22$)[8] it was found that Pb^{2+} ions are not randomly distributed over all the crystallographic sites but fill up only the tetragonal sites. More recently, the possibility of also occupying the pentagonal sites has been reported for the case when the number of lead ions is in excess of the number of tetragonal sites.[9] For the $x=0$ system this occurs at $y=0.33$ and for $x=0.75$ at $y=0.238$. As a result, a change in the slope of the cell-parameter variation can be expected and is indeed observed at the predicted y-values for both $x=0$ and $x=0.75$ systems (Fig. 3).

An analysis of microwave-dielectric properties shows that in the case of low x-values ($x=0.75$ and $x=0$) the maximum values of Q are observed on the Q vs. y plot (Fig. 4a). The Pb^{2+} concentrations associated with these maxima increase when the x-value decreases. According to previous studies,[10,11] the presence of these maxima

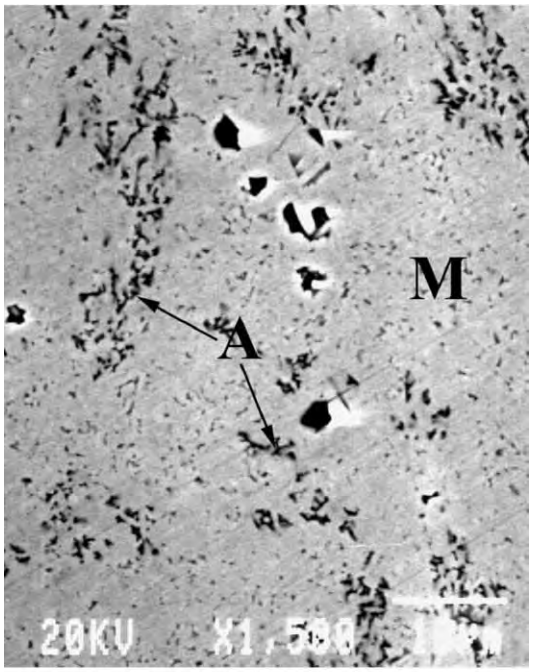

(a)

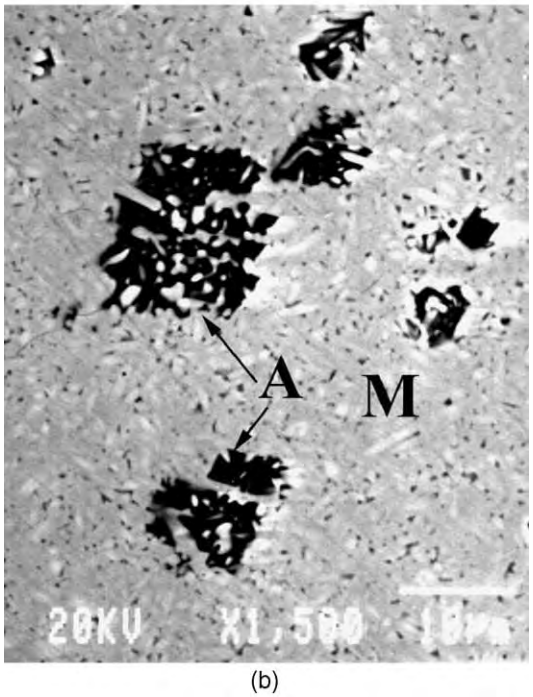

(b)

Fig. 3. SEM micrographs of $(Ba_{1-y}Pb_y)_{6-x}Nd_{8+2x/3}Ti_{18}O_{54}$ ($x=0.75$); M, matrix phase; A, secondary phase TiO_2 (rutile). (a) back-scattered electrons $y=0.3$; (b) back-scattered electrons $y=0.5$.

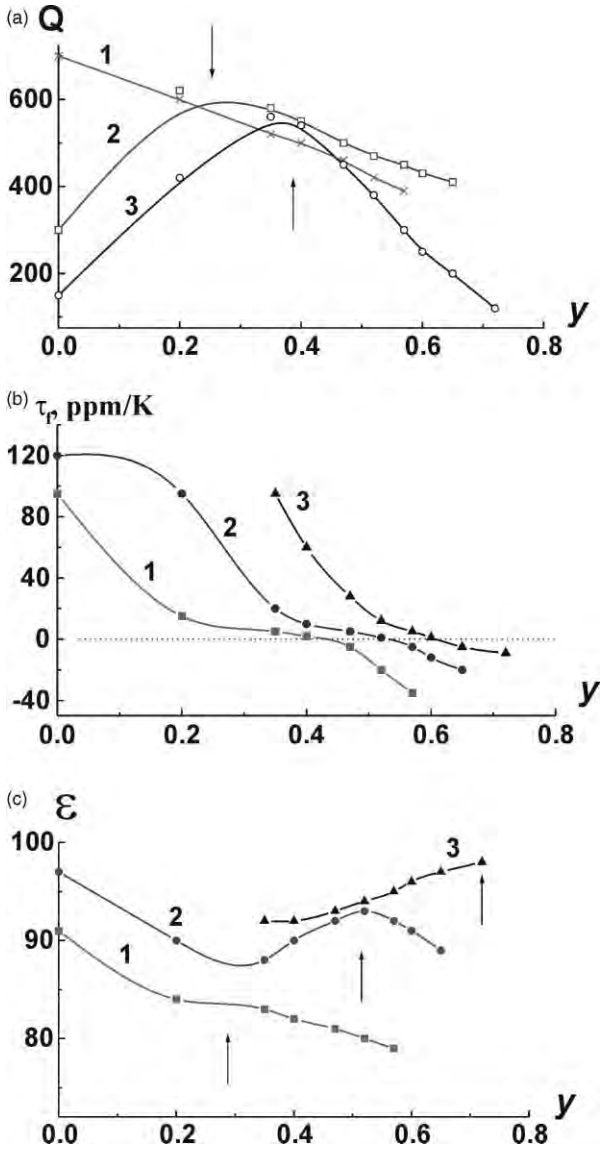

Fig. 4. Dielectric characteristics: (a) Q-value; (b) temperature coefficient of resonant frequency (τ_f); (c) dielectric constant (ϵ) of the $(Ba_{1-y}Pb_y)_{6-x}Nd_{8+2x/3}Ti_{18}O_{54}$ system as a function of Pb concentration, measured at 10 GHz. (1) $x=1.5$; (2) $x=0.75$; (3) $x=0$.

may be associated with the distribution of Pb^{2+} ions at different crystal sites (tetragonal and pentagonal sites in the A-sublattice) affecting the internal strain of the crystal lattice. The maximum Q values occur at lead concentrations which correspond to the complete substitution of Ba on the tetragonal sites according to the structural formulae $[Nd_8Pb_2][Ba_4]Ti_{18}O_{54}$ ($x=0$; $y=0.33$) and $[Nd_{8.5}\ Pb_{1.25}V_{0.25}][Ba_4]Ti_{18}O_{54}$ ($x=0.75$; $y=0.24$). The Ba^{2+} and Pb^{2+} ions are separated on different crystal sites, residing in pentagonal and tetragonal sites, respectively, and the lattice strain has its lowest value.[10] When $x=1.5$ the composition meets the above requirement at $y=0.11$. However, a maximum Q-factor is not observed on the plot of $Q(y)$. In the $Ba_{6-x}Nd_{8+2x/3}Ti_{18}O_{54}$ system the internal strain is the lowest at $x=1.5$,[1,2,9,10] which is the most probable reason why the lead substitution results only in a decrease in the Q-value, and that no maximum for Q is observed (Fig. 4a, curve 3). It should be noted that the presence of the secondary TiO_2 phase cannot influence the observed variations in the Q-values because of the very low dielectric losses of TiO_2.

The temperature coefficient of resonant frequency reaches zero ppm/K in the $(Ba_{1-y}Pb_y)_{6-x}Nd_{8+2x/3}Ti_{18}O_{54}$ system for all studied compositions ($x=0$, 0.75 and 1.5). The lower the value of x, the higher is the lead concentration which corresponds to a zero ppm/K value for τ_f. At the specific Pb^{2+} concentrations which correspond to the complete occupation of the tetragonal sites, deviations from linear behaviour are observed on the plots of τ_f vs. lead concentration (Fig. 4b). In addition, the temperature coefficient of resonant frequency decreases monotonically in all systems. It should be noted that according to Podlipnik et al.,[5] the τ_f reaches a minimum with increasing lead concentration, but in the present study this minimum was not observed. The discrepancy may be related to the different precursors used, which can effect the level of PbO evaporation and consequently the phase composition.

The dielectric constant in the $(Ba_{1-y}Pb_y)_{6-x}Nd_{8+2x/3}Ti_{18}O_{54}$ system changes only slightly with the lead concentration within the single-phase region (Fig. 4c). It varies by 5–7% whereas the other characteristics (ε and τ_f) display a much stronger variation. Interestingly, with increasing lead concentration the dielectric constant changes its behaviour: it decreases for low lead concentrations and increases at higher concentrations. On the $\varepsilon(y)$ plot, deviations from linear behaviour are observed at the lead concentration corresponding to the complete substitution of barium ions at the tetragonal sites (Fig. 4c), and as such can be ascribed to the different site occupation of Pb^{2+} ions.

3.2. The $(Ba_{1-y}Pb_y)_{6-x}La_{8+2x/3}Ti_{18}O_{54}$ system

The experimental work described in Section 3.1 shows that the concentrations of Pb^{2+} ions which correspond to the solid-solubility limits of $(Ba_{1-y}Pb_y)_{6-x}Nd_{8+2x/3}Ti_{18}O_{54}$ are in all cases higher than the concentrations needed for complete suppression of τ_f. In accordance with this fact there is an expectation that even higher τ_f-values can be suppressed to near zero ppm/K by Pb-doping. A possible candidate is the $Ba_{6-x}La_{8+2x/3}Ti_{18}O_{54}$ system with significantly higher permittivity (110 for $x=1.5$) but also a higher τ_f (450 ppm/K for $x=1.5$).

The X-ray diffraction pattern of the $(Ba_{1-y}Pb_y)_{6-x}La_{8+2x/3}Ti_{18}O_{54}$ powders ($x=0.75$) is presented in Fig. 5. The results of a comparative XRD phase analysis of the $(Ba_{1-y}Pb_y)_{6-x}Ln_{8+2x/3}Ti_{18}O_{54}$ materials indicates that for equal x-values the solid-solubility limits of Pb^{2+} ions are lower in the case of Ln = La than for Ln = Nd, and correspond to $y \approx 0.35$ (0.4) at $x=1.5$; $y \approx 0.45$ (0.6) at $x=0.75$; $y \approx 0.5$ (0.7) at $x=0$. The data related to the Nd-analogue are shown in the brackets.

At high lead concentrations in the $(Ba_{1-y}Pb_y)_{6-x}La_{8+2x/3}Ti_{18}O_{54}$ system a secondary phase appears, the peaks of which correspond to the composition $La_2Ti_3O_9$ ($La_{2/3}TiO_3$). $La_2Ti_3O_9$ is a metastable perovskite compound and known to decompose in oxidizing atmospheres above 800 °C forming $La_2Ti_2O_7$ and $La_4Ti_3O_{24}$.[12–14] However, the perovskite structure of $La_2Ti_3O_9$ can be stabilized in the environment of other perovskites, in particular $CaTiO_3$ and $PbTiO_3$.[14,15] Hence, the peaks of the secondary phase observed on the diffraction patterns at high lead concentrations may be assumed to correspond to the $La_2Ti_3O_9$ phase stabilized by $PbTiO_3$.

Crystal-lattice parameters of the $(Ba_{1-y}Pb_y)_{6-x}La_{8+2x/3}Ti_{18}O_{54}$ system linearly decrease with lead concentration within the single-phase region. The changes in this trend at $y \approx 0.35$, $x=1.5$; $y \approx 0.45$, $x=0.75$, and $y \approx 0.5$, $x=0$, correspond to the solubility limits of Pb^{2+} in the $(Ba_{1-y}Pb_y)_{6-x}La_{8+2x/3}Ti_{18}O_{54}$ system. Interestingly, in the case of La-containing systems, unlike Nd-containing systems, there are no deviations from the linear

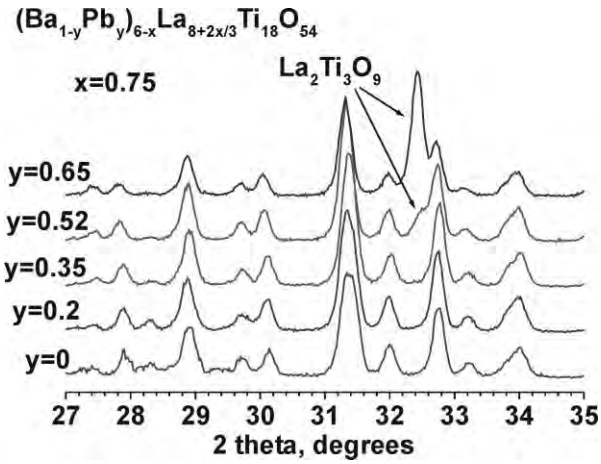

Fig. 5. X-ray diffraction patterns of the $(Ba_{1-y}Pb_y)_{6-x}La_{8+2x/3}Ti_{18}O_{54}$ system ($x=0.75$).

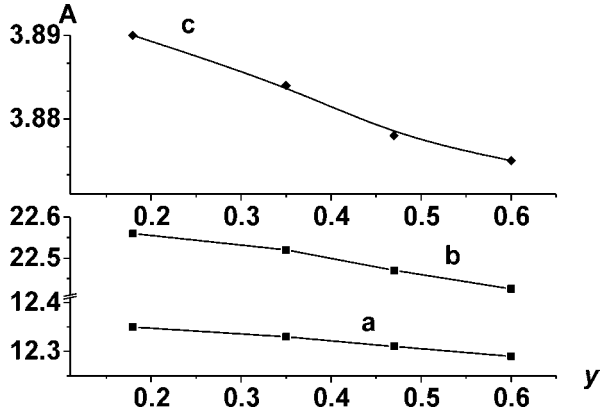

Fig. 6. Lattice parameters of the $(Ba_{1-y}Pb_y)_{6-x}La_{8+2x/3}Ti_{18}O_{54}$ system with $x=0$ as a function of Pb^{2+} concentration.

behaviour on the plots of the lattice parameters vs. lead concentration (Fig. 6).

The measured microwave dielectric properties (ε, τ_f, Q) of the $(Ba_{1-y}Pb_y)_{6-x}La_{8+2x/3}Ti_{18}O_{54}$ system are shown in Fig. 7. With increasing Pb^{2+} concentration the τ_f monotonically decreases, attains a minimum of about 200–300 ppm/K but never reaches a near-zero pmm/K (Fig. 7a). The dielectric constant (ε) shows behaviour similar to τ_f; it decreases with Pb concentration in the single-phase region and increases at higher lead concentrations as a result of the increase in the concentration of the $La_2Ti_3O_9$ secondary phase (Fig. 7b).

Unlike the Nd-analogue, the Q-values do not exhibit maxima in the Q vs. y plots (Fig. 7c). When increasing the concentration of Pb^{2+} ions in the single-phase region, the Q-values non-linearly increase for all x-values ($0 \geqslant x \geqslant 1.5$). The maxima in Q-values, which for Nd-analogues are ascribed to the change in the Pb-distribution, are in the case of the La-analogue not observed, probably due to the larger ionic radius of La^{3+} in comparison with Nd^{3+}.

3.3. The $(Ba_{1-y}Ca_y)_{6-x}Sm_{8+2x/3}Ti_{18}O_{54}$ system

Within the family of the $Ba_{6-x}Ln_{8+2x/3}Ti_{18}O_{54}$ compositions, the Sm-analogue is the material with one of the highest Q-values ($Q\times f \sim 10\,000$ GHz for $x=1.8$).[1–6,16,17] Together with a relatively high dielectric constant ($\varepsilon \approx 70$–80) it is also distinguished by a slightly negative temperature coefficient of resonant frequency which makes $Ba_{6-x}Sm_{8+2x/3}Ti_{18}O_{54}$-based ceramics an important material for utilization in the UHF region. The slightly negative τ_f of the $Ba_{6-x}Sm_{8+2x/3}Ti_{18}O_{54}$ solid solutions can be shifted towards zero by partial isovalent substitution of earth-alkaline elements, e.g. Sr or Ca for Ba.[3,6,11,17,18] Previously, during an investigation of the $(Ba_{1-\alpha}Sr_\alpha)O$–$Sm_2O_3$–$4.7TiO_2$ system, which is outside the homogeneity region, an increase in ε and τ_f with the strontium content was observed.[17] For $\alpha=0.05$ the material exhibited $\tau_f=0$, $\varepsilon=80$, and $Q\times f=11\,000$.[17]

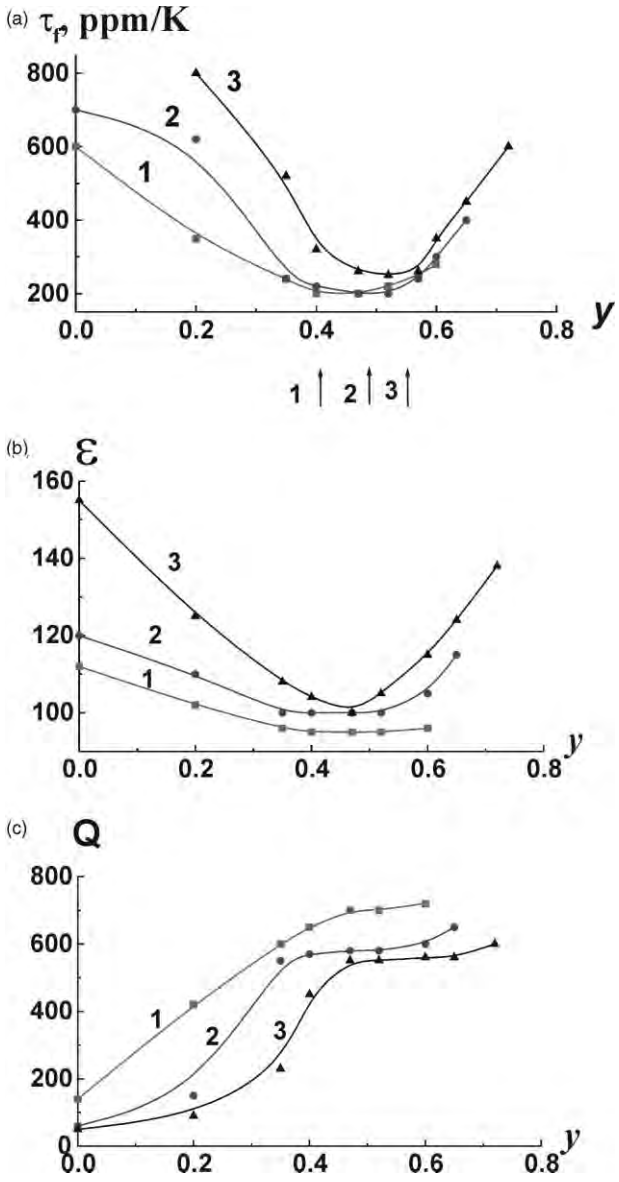

Fig. 7. Dielectric characteristics: (a) temperature coefficient of resonant frequency (τ_f); (b) dielectric constant (ε); (c) Q-value of the $(Ba_{1-y}Pb_y)_{6-x}La_{8+2x/3}Ti_{18}O_{54}$ system as a function of Pb concentration, measured at 10 GHz. (1) $x=1.5$; (2) $x=0.75$; (3) $x=0$.

When investigating the $(Ba,Sr)_{6-x}Sm_{8+2x/3}Ti_{18}O_{54}$ system for $x=1.8$, a near-zero τ_f was also achieved, however, at $\alpha=0.2$ when $Q\times f$ was as low as 3000.[11] The maximum $Q\times f$ ($Q\times f=10\,500$ GHz) has been reached at much higher strontium concentrations $\alpha=0.05$.

In addition to Sr-, also Ca-substituted systems (e.g. $(Ba_{1-x}Ca_x)O$–Sm_2O_3–$4.5TiO_2$)[6] show the increase of τ_f towards positive values. The changes observed in τ_f were ascribed to the presence of anomalies in the temperature dependence of the dielectric constant[6] which were first revealed for the Sm-analogue.[18] When increasing the calcium content in the $(Ba_{1-x}Ca_x)O$–Sm_2O_3–$4.5TiO_2$ system the maximum of ε was found to shift towards lower temperatures, effecting the τ_f value in the vicinity of

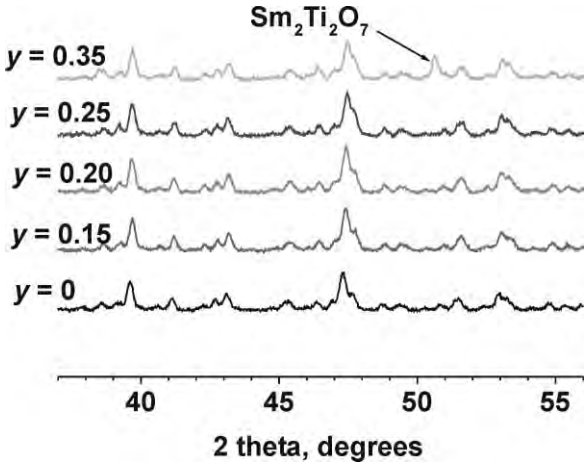

Fig. 8. X-ray diffraction patterns of the $(Ba_{1-y}Ca_y)_{6-x}Sm_{8+2x/3}Ti_{18}O_{54}$ system ($x=1.0$).

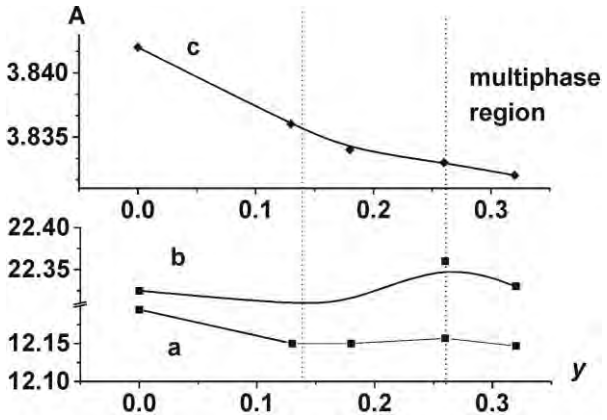

Fig. 9. Lattice parameters of the $(Ba_{1-y}Ca_y)_{6-x}Sm_{8+2x/3}Ti_{18}O_{54}$ system with $x=1.0$ as a function of Pb^{2+} concentration.

room temperature.[6] The reasons for the anomalies observed in the temperature dependence of the dielectric constant are not yet understood. There are also no microwave dielectric data for the compositions from the $(Ba,Ca)_{6-x}Sm_{8+2x/3}Ti_{18}O_{54}$ homogeneity range, although it is possible that we would expect lower dielectric losses compared to the Sr-substituted system due to the difference between the ionic radii, which is smaller in the case of Ca^{2+} and Ba^{2+} than for Sr^{2+} and Ba^{2+}. This conclusion initiated the investigations of the $(Ba_{1-y}Ca_y)_{6-x}Sm_{8+2x/3}Ti_{18}O_{54}$ system ($x=1.0$, and $x=1.5$) which are presented in this study.

The XRD analysis revealed the homogeneity regions of the $(Ba_{1-y}Ca_y)_{6-x}Sm_{8+2x/3}Ti_{18}O_{54}$ systems to be within $0\leqslant y<0.30$ for $x=1.0$ and $0\leqslant y<0.20$ for $x=1.5$. Above these Ca^{2+} concentrations, faint peaks of a secondary phase, which was identified as $Sm_2Ti_2O_7$, appear on the XRD patterns. A typical sequence of patterns is shown in Fig. 8 for the $x=1.0$ system. The lattice parameters of $(Ba_{1-y}Ca_y)_{4.5}Sm_9Ti_{18}O_{54}$ ($x=1.5$) linearly decrease with y within the solid-solubility limits whereas those of $(Ba_{1-y}Ca_y)_5Sm_{8.66(6)}Ti_{18}O_{54}$ ($x=1.0$) show slight deviations from linear dependence for $0.15\leqslant y\leqslant 0.20$ and especially at $0.25\leqslant y$ (Fig. 9). The latter deviation can be explained in terms of solid-solubility being exceeded and the former by the change in the Ca distribution. Initially, Ca^{2+} ions substitute for Ba^{2+} on tetragonal sites corresponding to the structural formulae $[Sm_9Ba_{0.5-4.5y}Ca_{4.5y}V_{0.5}][Ba_4]Ti_{18}O_{54}$ ($x=1.5$; $y\leqslant 0.11$), and $[Sm_{8.66(6)}Ba_{1-5y}Ca_{5y}V_{1/3}][Ba_4]Ti_{18}O_{54}$ ($x=1.0$; $y\leqslant 0.20$). For the incorporation of higher Ca concentrations the substitutional mechanism must change according to the structural formulae $[Sm_9Ca_{4.5y}V_{1.0-4.5y}][Ba_{4.5-4.5y}V_{4.5y-0.5}]Ti_{18}O_{54}$ and $[Sm_{8.66(6)}Ca_{5y}V_{4/3-5y}][Ba_{5-5y}V_{5y-1}]Ti_{18}O_{54}$.[10,11] As a result, the change in the substitutional mechanism influences the slope of the lattice parameters vs. y plot as seen in Fig. 9.

Dielectric characteristics (ε, τ_f, Q) as a function of the calcium concentration are shown in Fig. 10. With an increasing content of Ca^{2+} τ_f increases monotonically and attains maximum values in the vicinity of $y\approx 0.10$ ($x=1.5$) and $y\approx 0.2$ ($x=1.0$) (Fig. 10a). However, unlike the results reported earlier,[6,11,17] τ_f never attains zero values for both the investigated $(Ba_{1-y}Ca_y)_{6-x}Sm_{8+2x/3}Ti_{18}O_{54}$ systems. Most probably, the reason for the discrepancy with the published data is that the systems investigated previously do not belong to the $(Ba_{1-y}Ca_y)_{6-x}Sm_{8+2x/3}Ti_{18}O_{54}$ homogeneity region. The zero and even the positive τ_f reported could be ascribed to the presence of secondary phases, which in these cases would be TiO_2 and $BaTi_4O_9$, both distinguished by high positive τ_f values. The maximum τ_f in the $(Ba_{1-y}Ca_y)_{4.5}Sm_9Ti_{18}O_{54}$ ($x=1.5$) and $(Ba_{1-y}Ca_y)_5Sm_{8,66(6)}Ti_{18}O_{54}$ systems ($x=1.0$) is obtained at Ca concentrations corresponding to the complete substitution of all Ba^{2+} ions at the tetragonal sites by Ca^{2+} ions. Any further increase in Ca concentration, which is accompanied by a change in the substitutional mechanism, results in a decrease of τ_f.

Measurements of the dielectric constant as a function of temperature in the range of 20–200 °C revealed anomalies similar to those already described in the literature.[6,18] However, detailed analysis revealed additional phenomena which have not been described for a multiphase system. The temperature corresponding to the maximum dielectric-constant value shifts towards low temperatures with the increase of Ca concentration up to $y\approx 0.2$ ($x=1.0$), but it exhibits the opposite behaviour at higher calcium concentrations—a shift back to higher temperatures (Fig. 11). The same behaviour was also observed for the case of $x=1.5$. Such changes in the dielectric constant maximum can be induced by changes in the internal lattice strain resulting from a different Ca distribution.[10,11]

The dielectric constant of $(Ba_{1-y}Ca_y)_{6-x}Sm_{8+2x/3}Ti_{18}O_{54}$ decreases almost linearly for $x=1.5$ while for $x=1.0$

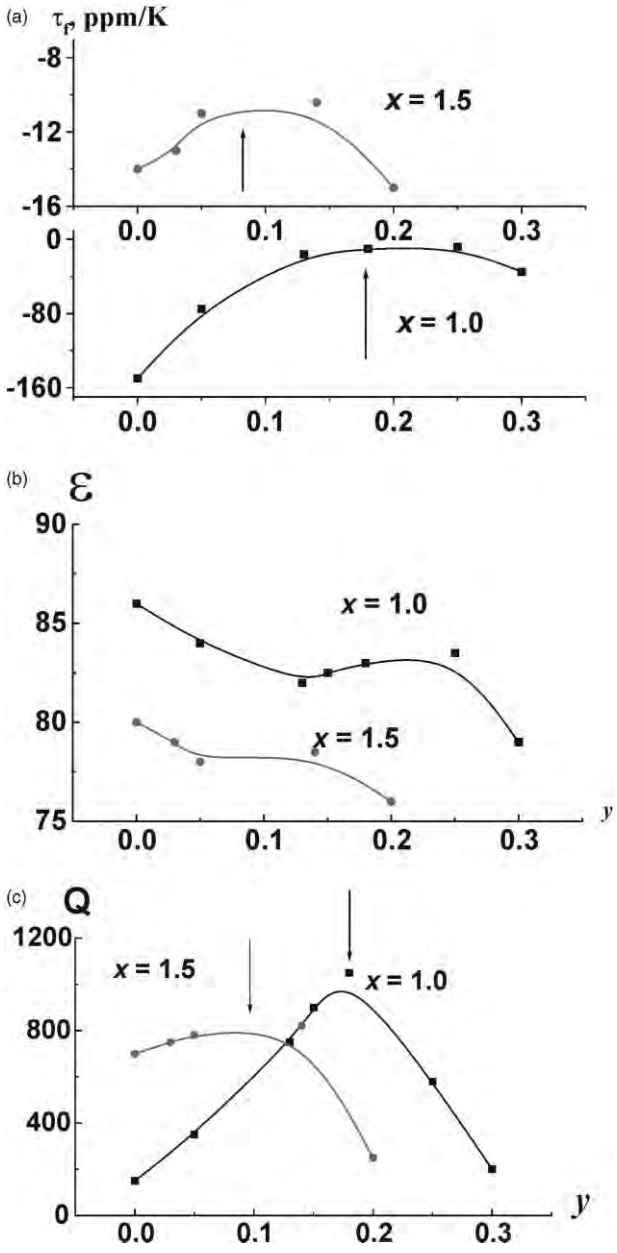

Fig. 10. Dielectric characteristics: (a) temperature coefficient of resonant frequency (τ_f); (b) dielectric constant (ε); (c) Q-value of the $(Ba_{1-y}Ca_y)_{6-x}Sm_{8+2x/3}Ti_{18}O_{54}$ system as a function of Ca concentration, measured at 10 GHz. (1)- $x=1.0$; (2)- $x=1.5$.

it slightly changes its trend at $0.15 \leqslant y \leqslant 0.20$ and begins to decrease at $0.25 \leqslant y$ (Fig. 10b). The behaviour of the dielectric constant is similar to that of the lattice parameters, and the direct relation between cell volume and dielectric-constant value, previously reported by many authors,[1,2,10,11] is confirmed in this case too.

Plots of Q vs. calcium concentration revealed maximums of Q for both compositions ($x=1.5$) and ($x=1.0$) (Fig. 10c). In both cases, maximum Q values are observed at calcium concentrations corresponding to complete substitution of the Ba^{2+} ions at tetragonal sites which can be ascribed to the lowest internal lattice strain

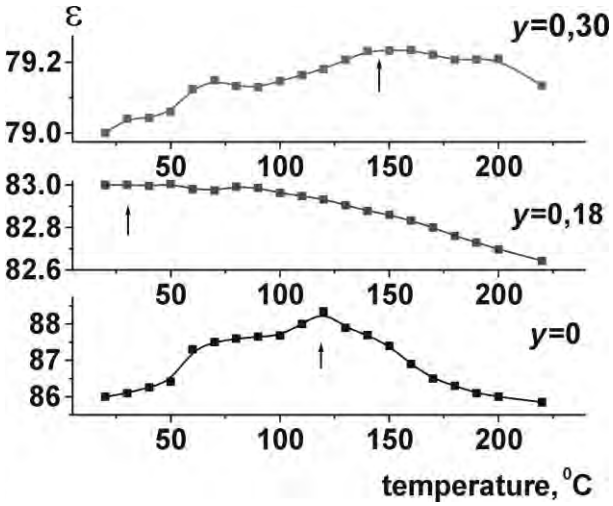

Fig. 11. Temperature dependence of the dielectric constant for $(Ba_{1-y}Ca_y)_5Sm_{8,6(6)}Ti_{18}O_{54}$ ($x=1.0$) as a function of Ca concentration.

attained when large Ba^{2+} and small (Sm^{3+} and Ca^{2+}) ions are separated at different crystallographic sites.[11]

4. Conclusions

Solid-solubility limits of solid solutions with the general formula $(Ba_{1-y}M_y)_{6-x}Ln_{8+2x/3}Ti_{18}O_{54}$ (Ln = La, Nd, Sm; M = Pb, Ca) have been determined for a wide range of y and x. The Pb^{2+} and Ca^{2+} ions, when partially substituting for Ba^{+2} ions, occupy first the tetragonal and then the pentagonal A-sites. Dielectric properties of the $(Ba_{1-y}M_y)_{6-x}Ln_{8+2x/3}Ti_{18}O_{54}$ (Ln = La, Nd, Sm; M = Pb, Ca) materials strongly depend on the distribution of the Pb^{2+} and Ca^{2+} ions at different crystallographic sites. By partial isovalent substitution of Pb^{2+} and Ca^{2+} for Ba^{+2} the temperature coefficient of resonant frequency (τ_f) of $Ba_{6-x}Ln_{8+2x/3}Ti_{18}O_{54}$ (Ln = La, Nd, Sm) can be significantly improved towards zero ppm/K. As a result, in the $(Ba_{1-y}Pb_y)_{6-x}Nd_{8+2x/3}Ti_{18}O_{54}$ system high-Q ceramic materials with τ_f of zero ppm/K and a dielectric constant of 90–100 have been produced.

References

1. Negas, T. and Davies, P. K., Influence of chemistry and processing on the electrical properties of $Ba_{6-3x}Ln_{8+2x}Ti_{18}O_{54}$ solid solutions, materials and processes for wireless communications. *Ceram. Trans.*, 1995, **53**, 179–192.
2. Ohsato, H., Mizuta, M., Ikoma, T., Onogi, Z., Nishigaki, S. and Okuda, T., Microwave dielectric properties of tungsten bronze-type $Ba_{6-3x}Nd_{8+2x/}Ti_{18}O_{54}$ (R = La, Pr, Nd, and Sm) solid solutions. *J. Ceram .Soc. Japan,* 1998, **106**(2), 178–182.
3. Nenasheva, E. A., Rotenberg, B. A., Gindin, E. I. and Prohvatilov, V. G., Dielectric properties and structure of titanates of rare-earth elements and alkaline-earth metals at isovalent substitutions in different sublattices. *Neorg. Mat.,* 1980, **16**(6), 1040–1043 (in Russian).

4. Wakino, K., Minai, K. and Tamura, H., Microwave characteristics of (Zr, Sn)TiO_4 and BaO–PbO–Nd_2O_3–TiO_2 dielectric resonators. *J. Am. Ceram. Soc.,* 1984, **67**(4), 278–282.
5. Podlipnik, M., Valant, M. and Suvorov, D., The influence of isovalent doping on the microwave dielectric properties of $Ba_{6-x}Nd_{8+2x/3}Ti_{18}O_{54}$ based ceramics. *Key Engineering Mater.,* 1997, **2**, 1211–1214.
6. Belous, A. G. and Ovchar, O. V., MW dielectrics with perovskite-like structure based on Sm-containing systems. *J. Eur. Ceram. Soc.,* 1999, **19**, 1119–1122.
7. Buzin, I. M. and Angelov, I. M., Dynamic measurement method of Q-factor and dielectric loss tangent in ferroelectrics in decimeter wavelength range. *Pribory, Technica, Ekspiriment,* 1974, **4**, 114–115 (in Russian).
8. Valant, M., Arčon, I., Suvorov, D., Kodre, A., Negas, T. and Frahm, R., Extended X-ray absorbtion fine structure study of incorporation of Bi and Pb atoms into the crystal structure of $Ba_{4.5}Nd_9Ti_{18}O_{54}$. *J. Mater. Res.,* 1997, **12**(3), 799–804.
9. Belous, A. G. and Ovchar, O. V., Pb-induced temperature stabilization of high dielectric constant in barium neodymium titanates. *Ferroelectrics,* 2000, **238**, 9–16.
10. Ohsato, H., Imaeda, M., Takagi, Y., Komura, A. and Okuda, T., Microwave quality factor improved by ordering of Ba and rare-earth on the tungsten bronze-type $Ba_{6-3x}Nd_{8+2x/}Ti_{18}O_{54}$ (R = La, Nd, and Sm) solid solutions. In *Proceedings of the Eleventh IEEE International Symposium on Applications of Ferroelectrics "ISAF XI"*, Vol. 129, Monterux, Switzerland, 1998, pp. 509–512.
11. Imaeda, M., Mizuta, M., Ito, K., Ohsato, H., Nishigaki, S. and Okuda, T., Microwave dielectric properties of $Ba_{6-3x}Sm_{8+2x/}Ti_{18}O_{54}$ solid solutions with Sr substituted for Ba. *Jpn. J. Appl. Phys.,* 1997, **36**(9B), 6012–6015.
12. Sych, A. M., Bilyk, D. I., Klemus, V. G. and Novik, T. V., Lanthanum, praseodymium and neodymium metatitanates. *Zh. Neorg. Khim.,* 1976, **21**(12), 3220–3223 (in Russian).
13. Abe, M. and Uchino, K., X-ray studies of deficient perovskite $La_{2/3}TiO_3$. *Mater. Res. Bull.,* 1974, **9**, 147–151.
14. Bazuev, G. V., Makarova, O. V. and Shveikin, G. P., Synthesis and X-ray investigation of the phases with variable composition $Ln_{2/3+x}TiO_{3-y}$ with perovskite structure. *Zh. Neorg. Khim.,* 1978, **23**(6), 1451–1455 (in Russian).
15. Nenasheva, E. A., Rotenberg, B. A., Boys, G. V., Gindin, E. I. and Ivanova, M. P., Structure and dielectric properties of the ceramics based on $PbTiO_3$–$La_2O_3 \times 3TiO_2$. *Neorg. Mat.,* 1979, **15**(3), 492–494 (in Russian).
16. Ohsato, H., Ohhashi, T., Kato, H. and Nishigaki, S., Microwave dielectric properties and structure of $Ba_{6-3x}Sm_{8+2x/}Ti_{18}O_{54}$ solid solutions. *Jpn. J. Appl. Phys.,* 1995, **34**(1P), 187–191.
17. Nishigaki, S., Kato, H., Yano, S. and Kamimura, R., Microwave dielectric properties of (Ba,Sr)O–Sm_2O_3–TiO_2 ceramics. *Am. Ceram. Soc. Bull.,* 1987, **66**(9), 1405–1410.
18. Butko, V. I., Belous, A. G. and Nenasheva, Y. A., Microwave dielectric properties of barium-llanthanide tetratitanates. *Fizyka Tvyordogo Tela,* 1984, **26**(10), 2951–2956 (in Russian).